

Coupled process of plastics pyrolysis and chemical vapor deposition for controllable synthesis of vertically aligned carbon nanotube arrays

Zhou Yang · Qiang Zhang · Guohua Luo ·
Jia-Qi Huang · Meng-Qiang Zhao · Fei Wei

Received: 21 December 2009 / Accepted: 3 June 2010
© Springer-Verlag 2010

Abstract Efficient conversion of waste plastics into advanced materials is of conspicuous environmental, social and economic benefits. A coupled process of plastic pyrolysis and chemical vapor deposition for vertically aligned carbon nanotube (CNT) array growth was proposed. Various kinds of plastics, such as polypropylene, polyethylene, and polyvinyl chloride, were used as carbon sources for the controllable growth of CNT arrays. The relationship between the length of CNT arrays and the growth time was investigated. It was found that the length of aligned CNTs increased with prolonged growth time. CNT arrays with a length of 500 μm were obtained for a 40-min growth and the average growth rate was estimated to be 12 $\mu\text{m}/\text{min}$. The diameter of CNTs in the arrays can be modulated by controlling the growth temperature and the feeding rate of ferrocene. In addition, substrates with larger specific surface area such as ceramic spheres, quartz fibers, and quartz particles, were adopted to support the growth of CNT arrays. Those results provide strong evidence for the feasibility of conversion from waste plastics into CNT arrays via this reported sustainable materials processing.

1 Introduction

Nanotechnology is the research on the control of matter at atomic or molecular scale. It has enormous potential to

create many new materials and devices with a vast range of applications. For example, the carbon nanotube (CNT) has become a kind of outstanding functional nanomaterials with its two-dimensional nanostructured tubular structure. The fantastic mechanical, electrical, and chemical properties of CNTs have motivated extensive research on the synthesis, purification, properties, and applications in composites, electronics, optics, energy conversion, and other fields of materials science [1–5]. According to their agglomerating behavior, CNTs can be divided into two kinds: CNT aggregates—in which CNTs are randomly entangled with each other and CNT arrays—in which CNTs are nearly parallel to each other. The CNT aggregates are powders which can be easily mass produced through fluidized bed catalytic chemical vapor deposition (CVD) [5]. However, they are difficult to disperse, which limits their further applications. While for the CNT arrays, they have many attractive properties such as ordered structure, unique anisotropic performances, identical tube length, uniform orientation, extra high purity, and can be easily spun into macroscopic fibers. The as-grown arrays can be used to construct field emission devices, anisotropic conductive materials, multi-functional membranes and super strong yarn. Even with the loss of the original alignment, longer and straighter multi-walled CNTs (MWCNTs) from the CNT arrays exhibit better performances than randomly aggregated multi-walled or even single-walled CNTs (SWCNTs) in the polymer reinforcements to improve its electrical, mechanical and thermal properties. These applications would be realized if a controllable route for the CNT array synthesis in a scalable way would be established with a low cost.

Until now, CVD has become the most efficient route to synthesize CNTs. Various hydrocarbons, such as acetylene [4], ethylene [6, 7], propylene [5], cyclohexane [8], xylene [9] etc. have been used as the carbon sources. Recent studies have demonstrated that natural materials can

Z. Yang · Q. Zhang · G. Luo (✉) · J.-Q. Huang · M.-Q. Zhao ·
F. Wei

Beijing Key Laboratory of Green Chemical Reaction Engineering
and Technology, Department of Chemical Engineering, Tsinghua
University, Beijing 100084, China
e-mail: luoguoh@fotu.org
Fax: +86-10-62772051

be used for the synthesis of CNTs, aiming at the development of low-cost, environmentally benign, and resource-saving processes for large-scale production [10–13]. Some natural carbon sources, such as turpentine oil [14–16], camphor [17], coal [18], liquefied petroleum gas [19–23], natural gas [24], city gas [11], are also effective for CNT growth. Exploring economic carbon sources for CNT growth is a flourishing area in the nanotechnology development.

On the other hand, it should be noticed that plastics have been widely used in our daily life with the fast development of petrochemical industry and plastic manufacture in the last century. This unavoidably impacts the environment as it causes a rapid increase in plastic waste. Up to now, waste plastics can be recycled through landfill, energy recovery, and mechanical recycling which recovers the plastic materials for similar or lower-quality applications [25–28]. Conspicuous environmental, social and economical benefits can be gained from the reuse of waste plastics. However, the above-mentioned methods show various disadvantages such as rising costs, the poor biodegradability and the possibility of unacceptable emissions. A great deal of attention is still drawn to the problem of finding an efficient way to reuse waste plastics. It should be noticed that plastics are polymerized from various hydrocarbons and their derivations. It would be a feasible route to reuse them if they could be converted into advanced materials (such as aligned CNTs) with high value and extraordinary performance via nanotechnology.

This contribution describes a detailed coupled process of plastic pyrolysis and chemical vapor deposition (CVD) to synthesize vertically aligned CNT arrays from a family of plastic, such as polypropylene (PP), polyethylene (PE), polyvinyl chloride (PVC). CNT arrays with good morphology can be successfully synthesized on certain substrates.

2 Experimental details

In a typical procedure, PP (2.0 g), ferrocene (0.1 g) laid in separate ceramic boats were fixed in different zones of a tubular quartz reactor with the inner diameter of one inch. Then the reactor was put into a three-stage electric furnace. The first stage is used for ferrocene sublimation by a rate of 0.1–0.8 g/min at 120–140°C for one minute. The second stage is for PP pyrolysis at 450°C. The third stage with an elevated temperature of 800°C is the CVD zone for CNT array growth. After 30-min growth, the furnace was cooled to room temperature naturally. Ar and H₂ were introduced into the reactor and maintained from the beginning to the end with a flow rate of 500 and 30 standard cubic centimeters per minute (sccm), respectively. The final product in the reactor was peeled off by blades for further characterization.

The morphology of the CNT arrays were obtained using a JSM 7401F scanning electron microscope (SEM) operated at 3.0 kV and a JEM 2010 transmission electron microscope (TEM) operated at 120.0 kV. The sample for the TEM observation was prepared using a common sonication method. Raman experiments were performed using a Renishaw RM2000 Raman spectrophotometer. The spectra were recorded using a He-Ne laser excited at 633.0 nm. The purity of the CNTs in the as-grown product was measured through thermal gravimetric analysis (TGA) by TGA Q500.

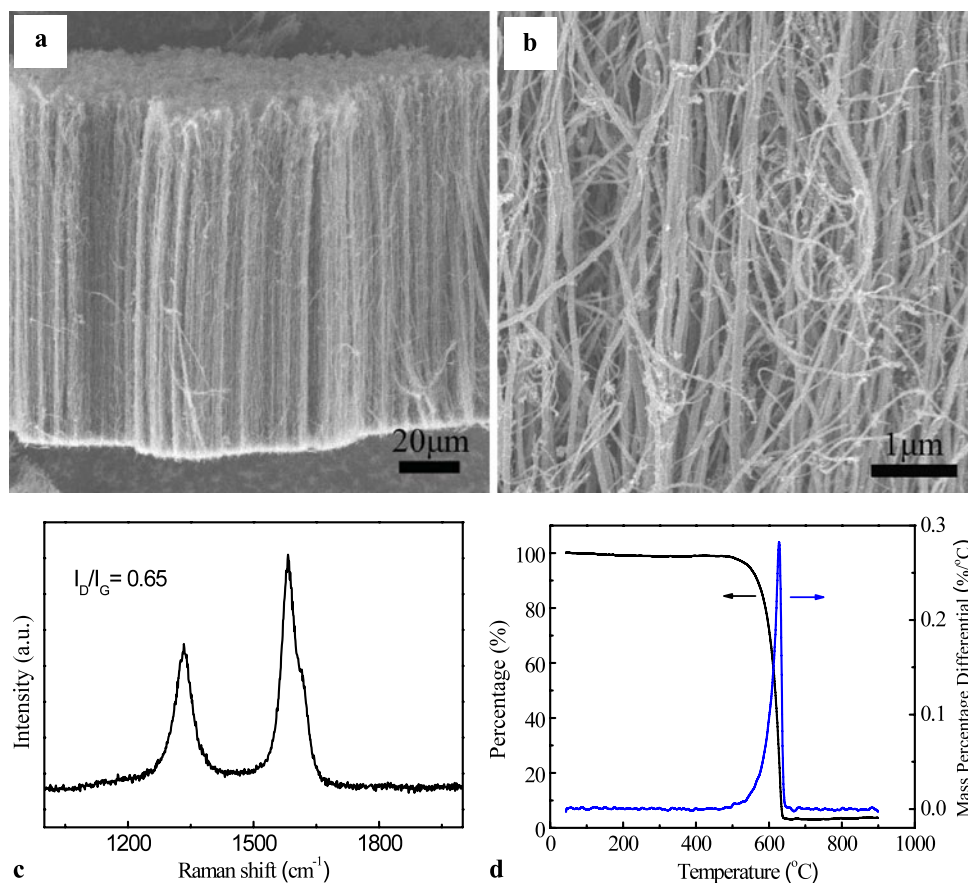
3 Results and discussion

3.1 Pyrolysis of PP into CNT arrays

The pyrolysis of PP results in a very complex product due to the high reaction temperature and the complicated free radical reactions involved. As was reported by Kruse et al. [29], the products of polypropylene cracking at 420°C included various alkanes, alkenes, alkynes, aromatics, and so on. About 36% were <C15 hydrocarbons, which can be easily delivered to the metal catalyst particles for the growth of CNT arrays. Some coke left as the residual after the pyrolysis as well. The gaseous products from pyrolysis of PP were introduced into the CVD zone with higher temperature by carrier gases and then CNT arrays grew through a CVD process. The as-grown product peeled off from the quartz substrate was in the state of a black free standing film. As is shown in Fig. 1a, the CNTs in the array are in a uniform orientation with a length of 100 μm. SEM images show the detailed structure of the CNT arrays, which consist of straight and curve CNTs (Fig. 1b). A typical Raman spectrum is illustrated in Fig. 1c. The two main peaks in 1580 cm⁻¹ (G peak) and 1350 cm⁻¹ (D peak) in the Raman spectra of the MWCNTs are the resonance peak of graphite and the scattering peak of disordered component, respectively. Therefore, the intensity ratio (I_D/I_G) is commonly used to characterize the crystallization degree of the samples. The value of I_D/I_G was 0.65, which indicated that the CNT arrays obtained from PP were with low defect density. From the TGA result of CNT arrays in Fig. 1d, it can be concluded that the purity of the CNT arrays was as high as 97.4%. Thus, it is feasible for the synthesis of CNT arrays with good alignment and high purity from PP.

A few other reports have described the growth of CNTs from polymers, such as PP [30–33] and PE [34–36]. However, only random entangled multi-walled CNTs were obtained [30–36]. The diameters of the as-obtained CNTs had a wide distribution. Compared with the previous reports [30–36], the fabrication of CNT arrays with ordered structure and extraordinary performance were realized herein. The production of CNT arrays from plastic route was attributed to the combination of plastic pyrolysis and CVD

Fig. 1 (a) SEM image, (b) high-resolution image, (c) Raman spectra and (d) TGA of CNT arrays grown from PP. Carbon source: 4.0 PP; catalyst precursor: 0.4 g/min ferrocene; growth time: 10 min; growth temperature: 800°C



growth on flat substrates in a reactor. In the present route, the catalyst particles formed through *in-situ* decomposition of ferrocene and the collision of iron atoms. The pyrolysis gas served as carbon source in the CVD process. The as-obtained iron particles were laid on the substrate [37] where the hydrocarbons of the pyrolysis gas decomposed into carbon atoms. Based on a vapor-liquid-solid CNT growth model [38], CNTs grew out when the carbon was supersaturated in iron particles. On a flat substrate, the initial as-grown CNTs formed a woven structure at the top of the array, and the following CNTs met large space resistance at the horizontal directions. Then the CNTs preferred growing vertically and formed an ordered array structure. The synchronous growth was mainly beneficial from the delicate interactions among CNTs [8]. Consequently, aligned CNTs were obtained from this sustainable material processing.

3.2 Modulation of the structures of CNT arrays

CNT arrays can be synthesized through the combination of pyrolysis of PP and a CVD process. The applications of CNT arrays were closely related to the structure, such as the length and diameter of CNTs. Here, we further provide the strategy to modulate the structure (length and diameter) of CNT arrays from the pyrolysis of plastic during the coupled process.

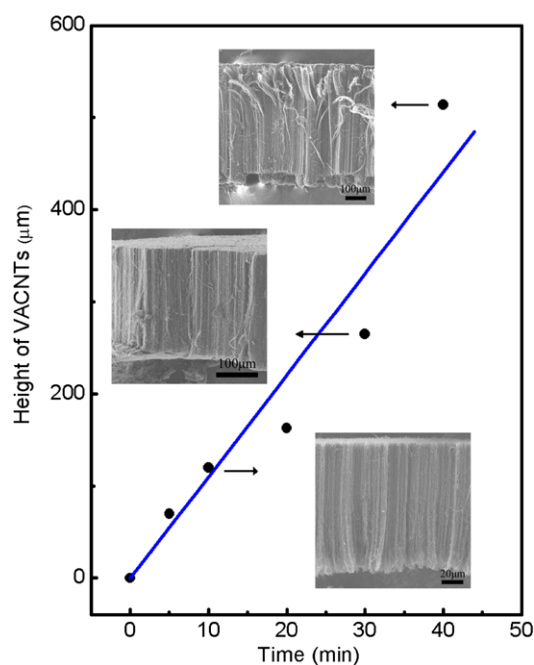


Fig. 2 The relationship between the growth time and length of CNT arrays grown at 800°C. Carbon source: 4.0 PP; catalyst precursor: 0.4 g/min ferrocene

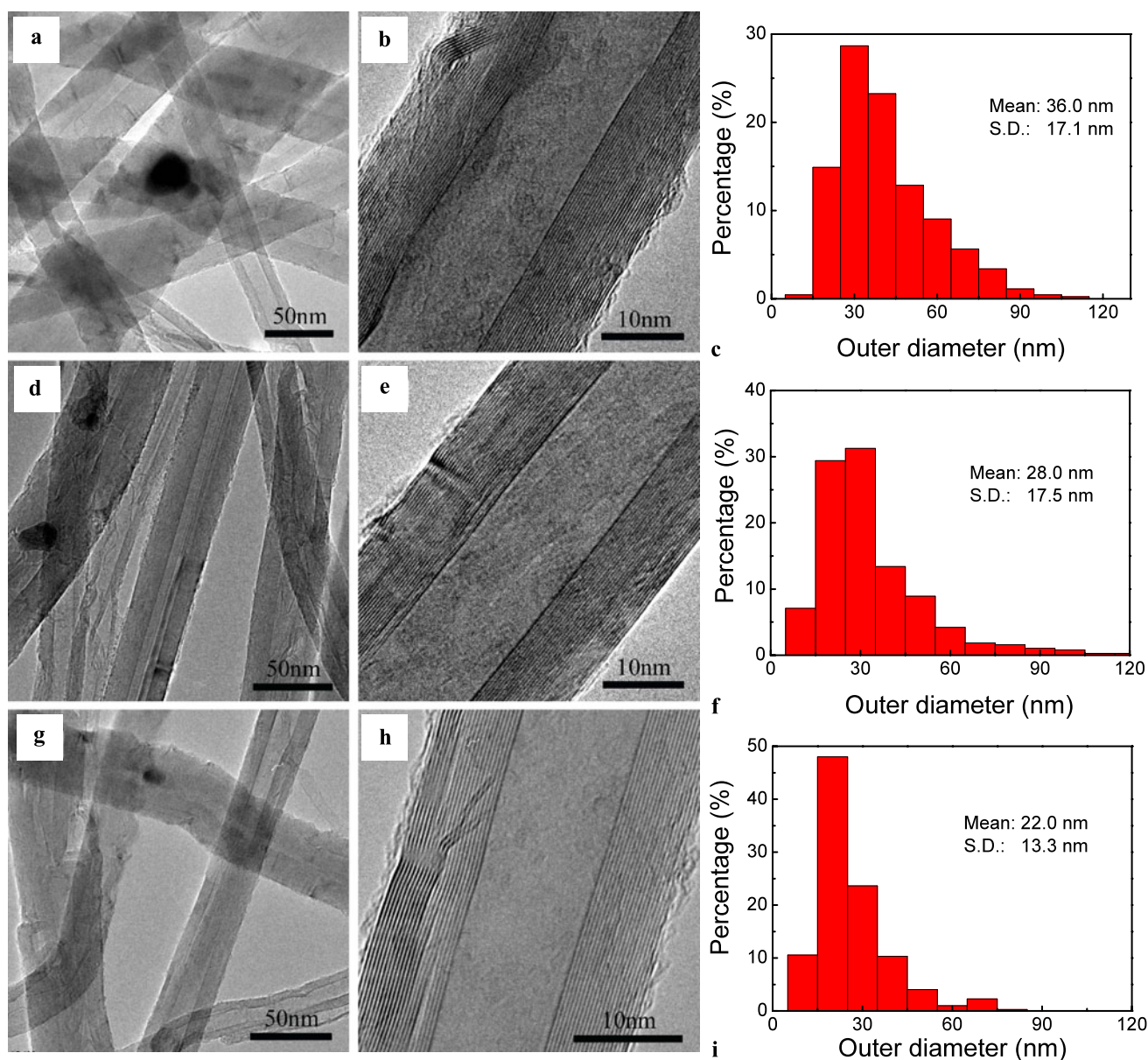


Fig. 3 TEM, high-resolution TEM images, and diameter distribution of CNTs in the array at different feeding rates of catalyst precursor: (a–c) 0.1 g/min; (d–f) 0.4 g/min; (g–i) 0.8 g/min. Carbon source: 4.0 PP; growth time: 30 min; growth temperature: 800°C

3.2.1 Modulating the length of CNT arrays

The length of CNT arrays can be easily modulated by varying the growth time. The length can be measured from the SEM image and the morphology evolution of the CNT arrays with the reaction time is shown in the inserted SEM images of Fig. 2. The length of CNT arrays increased almost linearly with the growth time within 40 min and the average growth rate was about 12 $\mu\text{m}/\text{min}$. This growth rate was lower than that of pure hydrocarbons, such as cyclohexane [8], xylene [9]. With the plastic serving as carbon source, the composition of the pyrolysis gas was complex. It was speculated that the decomposition rate of carbon source

on the surface of the catalyst particles was unstable, which led to a large fluctuation of carbon concentration in the catalyst particles, and reduced the growth rate of CNT arrays. After reacting for 40 minutes, the length of CNT arrays reached 500 μm . Due to the limited activity of the catalyst and the strong interactions among CNTs in the array, the synthesis of ultra-long CNT arrays was still an open question [39].

3.2.2 Modulating the diameter of CNTs in array

Many applications of CNT arrays were sensitive to the diameter of CNTs. The diameter distribution of the as-grown

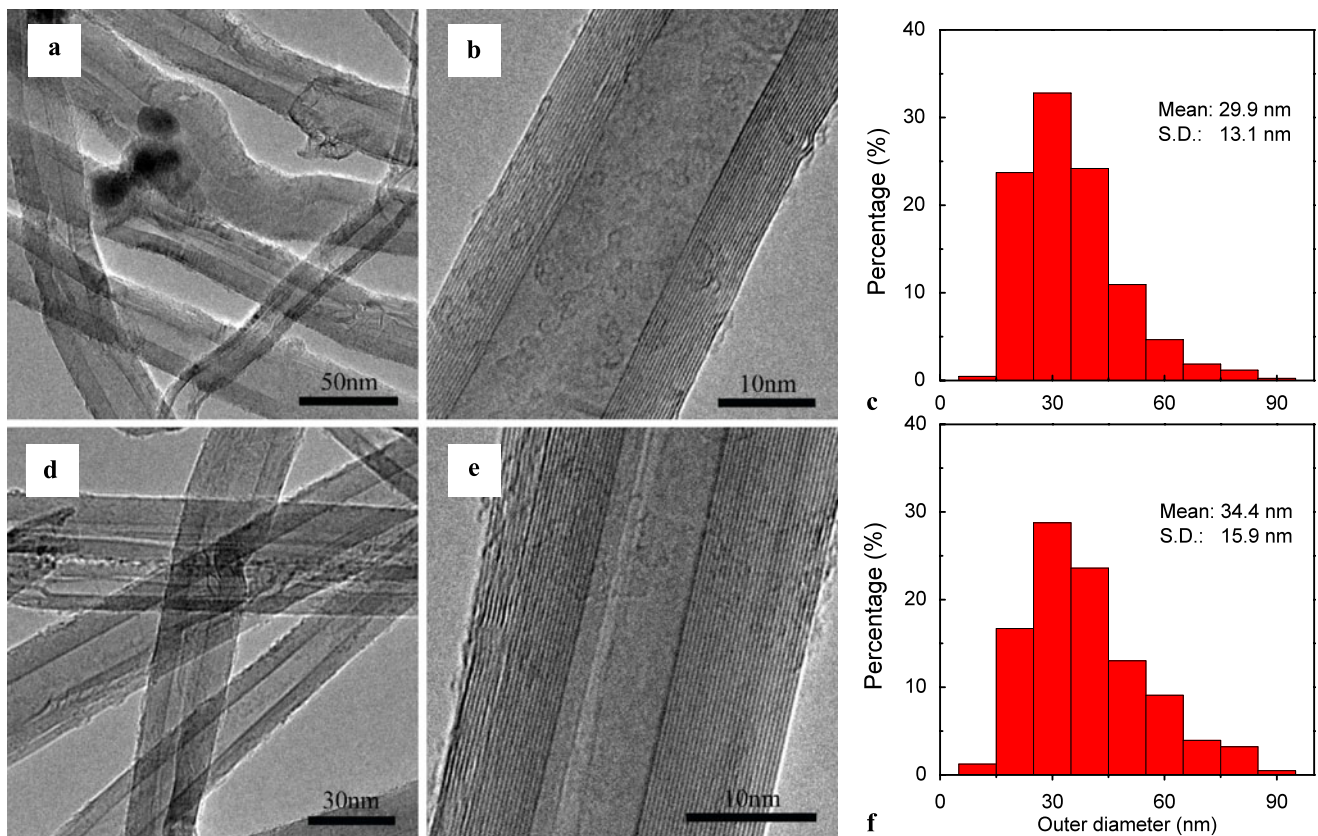


Fig. 4 TEM, high-resolution TEM images, and diameter distribution of CNTs in the array at different growth temperatures: (a–c) 800°C; (d–f) 850°C. Catalyst precursor: 0.2 g/min ferrocene; growth time: 30 min

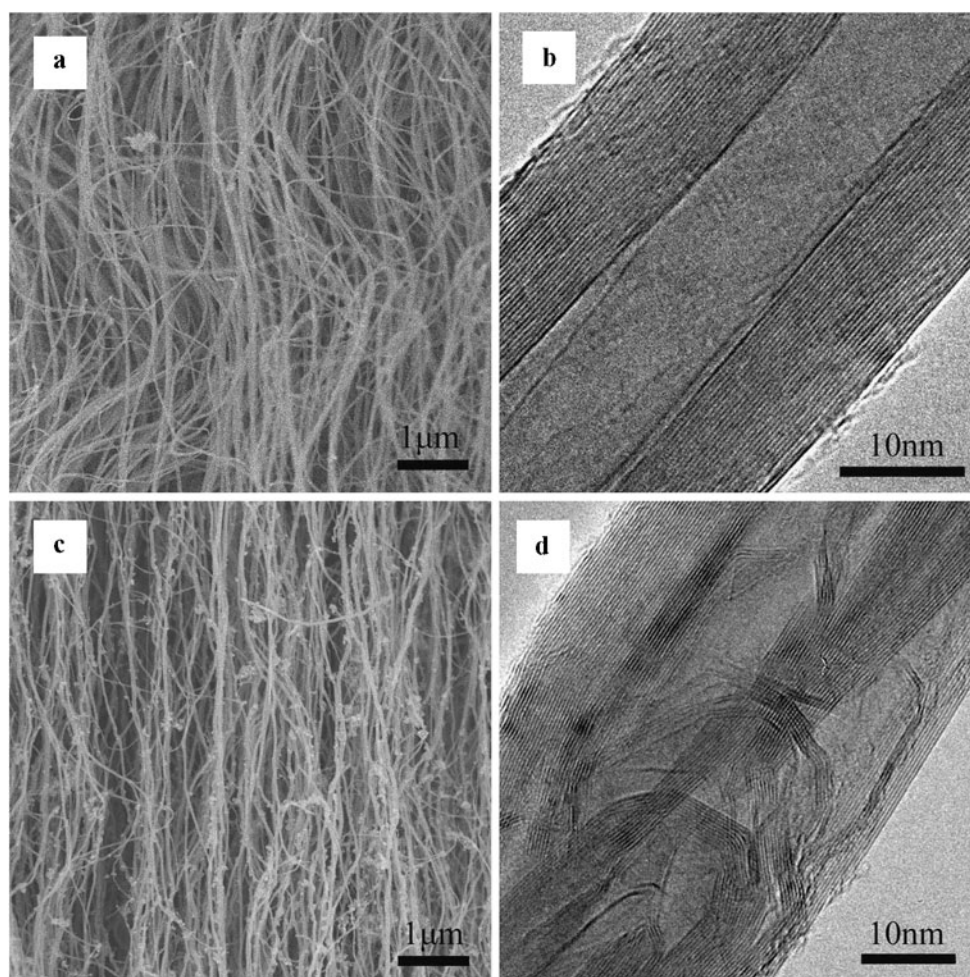
CNTs strongly depended on the size distribution of the catalyst particles. In the floating catalyst CVD process, the diameter of CNTs can be modulated by controlling the formation and assembling of catalyst particles, which were corresponding to the feeding rate of the catalyst precursor and the growth temperature.

Firstly, we modulated the catalyst particle formation by controlling the feeding rate of catalyst precursor. The feeding rate of ferrocene was varied to be 0.1 g/min, 0.4 g/min, and 0.8 g/min by increasing the evaporated temperature, with the fixed feeding rate of carbon source at 4.0 g/h. CNT arrays with good alignment grew on the inner surface of the quartz tube, and the related TEM images are illustrated in Fig. 3. All the products showed typical tubular structure. They presented a well-ordered structure with regularly distributed graphene layers. The diameter distribution varied with different feeding rates of catalyst precursor. With the feeding rate of 0.1 g/min, the diameter was in a wide range, and the mean diameter was 36.0 nm (Fig. 3c). When the feeding rate of catalyst precursor increased to 0.4 g/min, the mean diameter decreased to 28.0 nm (Fig. 3f). The mean diameter further decreased to 22.6 nm with a feeding rate of 0.8 g/min (Fig. 3i). The amount of ferrocene introduced into the reactor was about 100 times than the previous re-

ports [37]. A supersaturated state of iron atom was formed when the temperature was over 470°C. With higher saturation, the rate for the catalyst nucleation increased dramatically, leading to the formation of more particles with smaller sizes compared with the situation of lower saturation. As smaller catalyst particles were obtained, small diameter CNTs were synthesized consequently. This process for particle formation was similar to that for crystal growth in a saturation state.

After catalyst formation in the gas phase, the iron nanoparticles attached on the substrate, where further catalyst sintering took place. With varying growth temperature, the collision frequency in gas phase and sintering possibility on the substrate surface changed, resulting in the difference in the diameter of the iron catalysts and therefore the diameter of CNTs. Here, we fixed the feeding rate of catalyst precursor at 0.2 g/min, and the feeding rate of carbon source and the flow rate of carrier gases were fixed as well. Two different growth temperatures of 800°C and 850°C were evaluated, and the TEM images of the as-grown products are shown in Fig. 4. The as-grown products showed lower defect density under higher temperature. For CNT arrays that were grown at 800°C, the mean diameter was 29.9 nm, which increased to 34.4 nm when the

Fig. 5 SEM and high-resolution TEM images of CNT arrays from (a, b) PE and (c, d) PVC. Carbon source: 4.0 PE/PVC; catalyst precursor: 0.4 g/min ferrocene; growth time: 30 min; growth temperature: 800°C



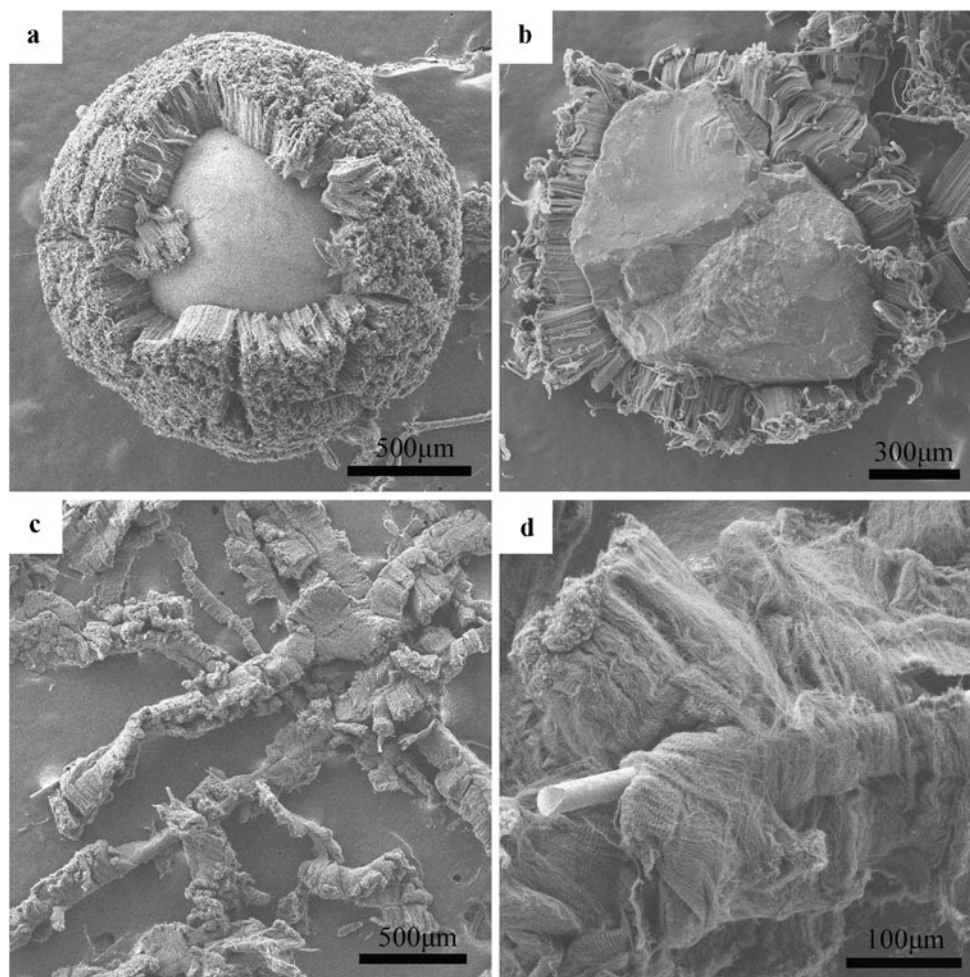
growth temperature was elevated to 850°C. A higher growth temperature increased the collision frequency in gas phase so that catalyst particles in larger size formed, and the sintering possibility also increased so that the small particles were prone to agglomerate into larger ones. As a result, the as-formed iron catalyst particles became larger in size and then CNTs with larger diameter in array form were synthesized.

3.3 Other plastics as carbon sources for CNT array growth

The present CNT array synthesis route was a versatile route to obtain advanced materials with certain structure from various plastics. Other plastics such as PE and PVC were also adopted for CNT array growth to demonstrate the generality of this approach. The pyrolysis products of PE mainly consisted of ethylene, ethane, butylene, butane, n-paraffine, vinyl olefin, et al. [40, 41]. Vertically aligned CNT arrays obtained from pyrolysis gas of PE are illustrated in Fig. 5. The as-grown product by PE showed a good morphology with clean surface (Fig. 5a). HRTEM image showed the ordered graphite layers of CNTs were with low defect den-

sity (Fig. 5b). During the pyrolysis of PVC, a more complex product with HCl (over 50%), liquid (benzene, alkyl aromatic, alkanes, etc.), gas fractions, carbon in residue, wax, and so on, were formed [42, 43]. The Cl element from PVC will partly poison the metal catalyst particles. Moreover, the Cl can bond with the dangling bonds of carbon or hydrogen [44]. Those are unfavorable for the normal dissolution of carbon in the iron phase and its precipitation at the carbon-metal interface to form CNTs [44–46]. Thus, the CNTs in the as-grown product derived from PVC entangled with each other more densely (Fig. 5c). HRTEM image revealed that the graphite layers were disordered and with high defect density (Fig. 5d). CNTs with disordered graphene layers were formed. No signal of Cl atoms can be detected on the as-grown products. The reason was attributed that the CNTs growth were in a mixture of Ar and H₂ at 800°C, the H₂ substitutes for Cl via the substitution reaction ($C-Cl + H_2 \rightarrow C-H + HCl$), and Cl element cannot be stably grafted on carbon [47–49]. Nevertheless, it is noticed that both PE and PVC can serve as a good carbon source for the growth of CNT arrays.

Fig. 6 SEM images of CNT arrays on different substrates: (a) ceramic sphere, (b) quartz particle, (c, d) quartz fiber. Carbon source: 4.0 PP; catalyst precursor: 0.4 g/min ferrocene; growth time: 30 min; growth temperature: 800°C



3.4 Other substrates in synthesizing CNT arrays from plastics

Furthermore, some novel substrates with large specific surface area, easy flow ability, and low cost were adopted for the growth of CNT arrays, such as spheres, fibers etc. Figure 6 shows CNT arrays grown on ceramic sphere, quartz fiber and particle. The surface of ceramic sphere was totally covered by radial CNT arrays (Fig. 6a). Similar with the growth on ceramic sphere [7], the surface of quartz particle was completely covered by CNT arrays (Fig. 6b). When CNT arrays were grown on the quartz fiber, they seemed like a brush because the shape of the quartz fiber was cylindrical with a diameter of 10 μm , so that CNT arrays tended to grow on the surface in an opposite direction and finally became a brush-like structure (Fig. 6c, d). The use of substrates with larger specific surface area was beneficial for the synthesis of CNT arrays at a large scale. Moreover, it should be noticed that some CNT arrays were released during the SEM sample preparation process, which was attributed to the stronger adhesion between carbon tape and CNT arrays than that between the iron catalyst and quartz substrate. Free

standing CNT arrays can be released on a large scale from various substrates by using CO_2 as an oxidative reagent to weaken the array-substrate interaction and facilitate their harvest [50].

Finally, it should be noticed that various kinds of plastics can serve as carbon sources for the growth of CNT arrays on the surface of spherical, fibrous, or flat substrates. This indicated that waste plastics (a mixture of various plastics) were also promising for the effective synthesis of CNT arrays at a large scale in the future. This is an easy way to transform waste into advanced materials through nanotechnology.

4 Conclusions

CNT arrays have been obtained through a pyrolysis-CVD coupled process with PP, PE and PVC as the carbon source and ferrocene as the catalyst precursor. With PP as the carbon source, the growth rate of CNT arrays is about 12 $\mu\text{m}/\text{min}$. The diameter of the CNTs can be modulated by controlling either the growth temperature or the feeding rate of catalyst precursor. Various kinds of plastics and various

substrates can be adopted for the synthesis of CNT arrays as well, indicating this approach to be a versatile method to convert plastics into CNT arrays. This provides a new route to recycle plastics into advanced materials through sustainable materials processing.

Acknowledgements The work was supported by the Foundation for Natural Science Foundation of China (No. 20606020, No. 20736004, and No. 20736007), China National Program (No. 2006CB0N0702).

References

- J. Zhang, X. Liu, R. Blume, A.H. Zhang, R. Schlogl, D.S. Su, *Science* **322**, 73 (2008)
- C.M. Rouleau, G. Eres, H. Cui, H.M. Christen, A.A. Puzos, D.B. Geohegan, *Appl. Phys. A* **93**, 1005 (2008)
- M. Maghrebi, A.A. Khodadadi, Y. Mortazavi, A. Sane, M. Rahimi, Y. Shirazi, Z. Tsakadze, S. Mhaisalkar, *Appl. Phys. A* **97**, 417 (2009)
- X.B. Zhang, K.L. Jiang, C. Teng, P. Liu, L. Zhang, J. Kong, T.H. Zhang, Q.Q. Li, S.S. Fan, *Adv. Mater.* **18**, 1505 (2006)
- F. Wei, Q. Zhang, W.Z. Qian, H. Yu, Y. Wang, G.H. Luo, G.H. Xu, D.Z. Wang, *Powder Technol.* **183**, 10 (2008)
- S.S. Fan, M.G. Chapline, N.R. Franklin, T.W. Tombler, A.M. Cassell, H.J. Dai, *Science* **283**, 512 (1999)
- Q. Zhang, J.Q. Huang, M.Q. Zhao, W.Z. Qian, Y. Wang, F. Wei, *Carbon* **46**, 1152 (2008)
- Q. Zhang, W.P. Zhou, W.Z. Qian, R. Xiang, J.Q. Huang, D.Z. Wang, F. Wei, *J. Phys. Chem. C* **111**, 14638 (2007)
- X.F. Zhang, A.Y. Cao, B.Q. Wei, Y.H. Li, J.Q. Wei, C.L. Xu, D.H. Wu, *Chem. Phys. Lett.* **362**, 285 (2002)
- D.S. Su, *ChemSusChem* **2**, 1009 (2009)
- M. Endo, K. Takeuchi, Y.A. Kim, K.C. Park, T. Ichiki, T. Hayashi, T. Fukuyo, S. Linou, D.S. Su, M. Terrones, M.S. Dresselhaus, *ChemSusChem* **1**, 820 (2008)
- D.S. Su, X.W. Chen, X. Liu, J.J. Delgado, R. Schlogl, A. Gajovic, *Adv. Mater.* **20**, 3597 (2008)
- M.Q. Zhao, Q. Zhang, J.Q. Huang, J.Q. Nie, F. Wei, *ChemSusChem* **3**, 453 (2010)
- R.A. Afre, T. Soga, T. Jimbo, M. Kumar, Y. Ando, M. Sharon, *Chem. Phys. Lett.* **414**, 6 (2005)
- P. Ghosh, T. Soga, M. Tanemura, M. Zamri, T. Jimbo, R. Katoh, K. Sumiyama, *Appl. Phys. A* **94**, 51 (2009)
- P. Ghosh, T. Soga, K. Ghosh, T. Jimbo, R. Katoh, K. Sumiyama, Y. Ando, *Nanoscale Res. Lett.* **3**, 242 (2008)
- M. Kumar, Y. Ando, J. Nanosci. *Nanotechnol.* **10**, 3739 (2010)
- Z.Y. Wang, Z.B. Zhao, J.S. Qiu, *Carbon* **44**, 1845 (2006)
- Q. Zhang, Y. Liu, J.Q. Huang, W.Z. Qian, Y. Wang, F. Wei *Nano*, **3**, 95 (2008)
- Q. Zhang, J.Q. Huang, F. Wei, G.H. Xu, Y. Wang, W.Z. Qian, D.Z. Wang, *Chin. Sci. Bull.* **52**, 2896 (2007)
- J.Q. Huang, Q. Zhang, F. Wei, W.Z. Qian, D.Z. Wang, L. Hu, *Carbon* **46**, 291 (2008)
- P. Ndungu, Z.G. Godongwana, L.F. Petrik, A. Nechaev, S. Liao, V. Linkov, *Micropor. Mesopor. Mater.* **116**, 593 (2008)
- J.M. Zhou, G.D. Lin, H.B. Zhang, *Catal. Commun.* **10**, 1944 (2009)
- R. Bonadiman, M.D. Lima, M.J. de Andrade, C.P. Bergmann, *J. Mater. Sci.* **41**, 7288 (2006)
- J. Walendziewski, *Fuel* **81**, 473 (2002)
- A.A. Garforth, S. Ali, J. Hernandez-Martinez, A. Akah, *Curr. Opin. Solid State Mater. Sci.* **8**, 419 (2004)
- J. Aguado, D.P. Serrano, J.M. Escola, *Ind. Eng. Chem. Res.* **47**, 7982 (2008)
- M.A. Keane, *ChemSusChem* **2**, 207 (2009)
- T.M. Kruse, H.W. Wong, L.J. Broadbelt, *Macromolecules* **36**, 9594 (2003)
- T. Tang, X.C. Chen, X.Y. Meng, H. Chen, Y.P. Ding, *Angew. Chem. Int. Ed.* **44**, 1517 (2005)
- U. Arena, M.L. Mastellone, G. Camino, E. Boccaleri, *Polym. Degrad. Stabil.* **91**, 763 (2006)
- Z.W. Jiang, R.J. Song, W.G. Bi, J. Lu, T. Tang, *Carbon* **45**, 449 (2007)
- J.H. Zhang, J. Li, H. Cao, Y.T. Qian, *Mater. Lett.* **62**, 1839 (2008)
- Q.H. Kong, J.H. Zhang, *Polym. Degrad. Stabil.* **92**, 2005 (2007)
- Y.W. Yen, M.D. Huang, F.J. Lin, *Diam. Relat. Mater.* **17**, 567 (2008)
- V.G. Pol, P. Thiyagarajan, *J. Environ. Monit.* **12**, 455 (2010)
- Q. Zhang, J.Q. Huang, M.Q. Zhao, W.Z. Qian, F. Wei, *Appl. Phys. A* **94**, 853 (2009)
- R.T.K. Baker, *Carbon* **27**, 315 (1989)
- E.R. Meshot, A.J. Hart, *Appl. Phys. Lett.* **92**, 113107 (2008)
- N. Miskolczi, A. Angyal, L. Bartha, I. Valkai, *Fuel Process. Technol.* **90**, 1032 (2009)
- A.A. Garforth, Y.H. Lin, P.N. Sharratt, J. Dwyer, *Appl. Catal. A* **169**, 331 (1998)
- Y. Masuda, T. Uda, O. Terakado, M. Hirasawa, *J. Anal. Appl. Pyroly.* **77**, 159 (2006)
- I.C. McNeill, L. Memetea, W.J. Cole, *Polym. Degrad. Stabil.* **49**, 181 (1995)
- Q. Zhang, H. Yu, J.Q. Huang, L. Hu, W.Z. Qian, D.Z. Wang, F. Wei, *Mater. Lett.* **62**, 3149 (2008)
- R.T. Lv, F.Y. Kang, D. Zhu, Y.Q. Zhu, X.C. Gui, J.Q. Wei, J.L. Gu, D.J. Li, K.L. Wang, D.H. Wu, *Carbon* **47**, 2709 (2009)
- R.T. Lv, S. Tsuge, X.C. Gui, K. Takai, F.Y. Kang, T. Enoki, J.Q. Wei, J.L. Gu, K.L. Wang, D.H. Wu, *Carbon* **47**, 1141 (2009)
- H. Tobias, A. Soffer, *Carbon* **23**, 281 (1985)
- H.P. Boehm, *Carbon* **32**, 759 (1994)
- A. Nakamura, T. Inui, N. Kinomura, T. Suzuki, *Carbon* **38**, 1361 (2000)
- J.Q. Huang, Q. Zhang, M.Q. Zhao, F. Wei, *Carbon* **48**, 1441 (2010)